Molecular Neurobiology

ISSN0893-7648/94/8(2–3): 105–112/$5.60

PrP in Pathology and Pathogenesis in Scrapie-Infected Mice

M. E. Bruce,*[1] P. A. McBride,[1] M. Jeffrey,[2] and J. R. Scott[1]

[1]*IAH AFRC & MRC Neuropathogenesis Unit, Ogston Building, West Mains Road, Edinburgh, EH9 3JF, UK; and* [2]*Lasswade Veterinary Laboratory, Bush Estate, Penicuik, Midlothian, EH26 OSA, UK*

Abstract

PrP accumulation in the brains of mice infected with scrapie takes several different forms: amyloid plaques, widespread accumulation in neuropile, and perineuronal deposits. PrP is also sometimes detected within microglia and in or around astrocytes. There are dramatic and reproducible differences between scrapie strains in the relative prominence of these changes and their distribution in the brain. Depending on the scrapie strain, PrP pathology is targeted precisely to particular brain areas, often showing a clear association with identifiable groups of neurons. These results suggest that PrP changes are primarily associated with neurons, and that different scrapie strains recognize and selectively replicate in different populations of neurons. Immunostaining at the ultrastructural level demonstrates an association of PrP with neurite plasmalemma, around amyloid plaques, and in areas of widespread neuropile and perineuronal accumulation. It is probable that PrP is encoded by the *Sinc* gene, which controls the incubation period of scrapie in mice. Studies using the intraocular infection route show that the *Sinc* gene controls the onset rather than the rate of replication, suggesting that PrP may be involved in cell-to-cell spread of infection. The accumulation of PrP at the surface of neurons is consistent with such a role.

Index Entries: Scrapie; PrP; scrapie strains; scrapie pathology; scrapie pathogenesis, mouse *Sinc* gene.

Introduction

It has become clear in recent years that the host protein, PrP, play a central role in the pathogenesis of scrapie and related diseases. Most obviously, PrP accumulates pathologically in the brains of infected animals in abnormally protease-resistant forms *(1)*. Aggregates of this protein can be detected in detergent-treated tissue extracts, negatively stained for electron microscopy, as scrapie-associated fibrils (SAF) *(2)*, or prion rods *(3)*. When visualized immunocytochemically in tissue sections *(4)*, PrP accumulations take a number of different morphological forms, including amyloid plaque cores and diffuse or granular neuropile deposits. Experimental studies of scrapie in mice have shown that the relative prominence of these changes and their distribution in the brain depend on the strain of agent *(5)*.

*Author to whom all correspondence and reprint requests should be addressed.

There are many strains of mouse-passaged scrapie, identified primarily from their incubation periods in genetically defined mice *(6)*. The incubation period of the disease is closely controlled by the mouse *Sinc* gene (scrapie incubation), two alleles of which have been identified, designated s7 and p7 *(7)*. The length of the incubation period for any particular model depends on specific and precise interactions between the *Sinc* genotype of the mouse and the strain of scrapie agent *(6)*. For a single scrapie strain, the *Sinc* genotype of the mouse can make an enormous difference in the incubation period; for example, for the 22A strain of scrapie, the incubation period is about 200 d in $Sinc^{p7}$ mice and about 450 d in $Sinc^{s7}$ mice.

One of the most interesting recent developments has been the recognition that the *Sinc* gene and the gene encoding PrP, *Prn-p*, are closely linked *(8,9)*. In all mouse strains so far tested, including *Sinc* congenic lines, the two known *Sinc* alleles (s7 and p7) are consistently associated with variants of PrP that differ by two amino acids. This strongly suggests that the *Sinc* gene encodes PrP and that the amino acid differences between the two variants of PrP are responsible for the biological effects of the *Sinc* gene. Thus, PrP appears to be closely involved in the genetic control by the host of the progression of the disease, as well as accumulating pathologically in the brain. In this article, we review some of our recent findings on PrP-related pathology, scrapie strain differences, and the action of the *Sinc* gene.

Methods

Three mouse-passaged scrapie strains showing contrasting patterns of pathology were used: 87V, which has been isolated and passaged in VM mice, and ME7 and 79A, which have been isolated and passaged in C57BL mice *(6)*. The pathology produced by these strains was studied in the following inbred mouse strains: C57BL and VM-$Sinc^{s7}$, which are homozygous for the s7 allele of *Sinc* (or the a allele of *Prn-p*), and VM, IM, and MB, which are homozygous for the p7 allele of *Sinc* (or the b allele of *Prn-p*). VM-$Sinc^{s7}$ is a *Sinc* congenic line derived from VM *(6,9)*. Mice were injected intracerebrally with 20 µL 1% mouse brain homogenates. After a long incubation period, differing between models, mice were killed at a standard clinical end point *(7)*. Age-matched mice, injected with uninfected brain homogenates, were included as controls in the pathological studies. In some experiments designed to investigate the progression of pathology, groups of mice were killed at intervals through the incubation period.

For the light microscopic study, as described previously *(5)*, brains were perfusion-fixed in periodate-lysine paraformaldehyde (PLP), trimmed at standard coronal levels, and embedded in paraffin wax. After removal of wax, sections were pretreated with 98% formic acid to enhance immunolabeling and immunostained by the peroxidase/anti-peroxidase (PAP) method with a polyclonal rabbit antiserum to mouse SAF (1B3) *(10)*. Control sections were incubated with preimmune serum in place of the primary antiserum.

For immunostaining at the ultrastructural level *(11)*, VM mice with 87V scrapie at a late stage in the disease were perfused with a 3% paraformaldehyde/1% glutaraldehyde mixture and blocks were dissected from areas of brain showing particular types of pathology. These were postfixed in osmium tetroxide and embedded in araldite. In order to correlate immunostaining patterns at the light and ultrastructural levels, serial 1-µm and 65-nm sections were cut from suitable blocks. For light microscopy, 1-µm sections were etched with saturated sodium ethoxide diluted 1:1 with ethanol, treated with 3% hydrogen peroxide in methanol to deplasticize and block endogenous peroxidase, and immunostained with 1B3 by the PAP method after enhancement with formic acid. For electron microscopy, 65-nm sections were etched with sodium periodate, deosmicated with 3% hydrogen peroxide in methanol, and pretreated with formic acid; they were then immunogold-labeled by incubating with the 1B3 antibody followed by Extravidin (Sigma diagnostics), postfixed with glutaraldehyde, and counterstained with uranyl acetate and lead citrate.

For the pathogenesis study *(12)*, VM and VM-$Sinc^{s7}$ mice were injected with 1 µL 1% ME7 inoculum into each eye. Mice were killed at intervals after injection, and the level of infectivity in the superior colliculi was estimated by incubation period assay. These assays were carried out by injecting groups of VM-$Sinc^{s7}$ mice with 10% homogenates, recording the incubation period in the mice, and reading off the level of infectivity in the inoculum from a standard dose–response curve.

Results and Discussion

PrP Detection in Uninfected Brain

1B3, like all other PrP-specific antibodies currently available, recognizes both the normal and abnormal forms of the protein *(10)*. In uninfected

brain, as previously described (5), immunolabeling of PrP was confined to some neuronal cell bodies. Labeling within these neurons had a punctate appearance, suggestive of a lysosomal distribution. Labeled neurons were seen throughout the brain, but were more frequent in some areas, such as the hippocampus. Large neuronal cell bodies, for example, those of Purkinje cells and hippocampal pyramidal cells, were particularly prominently stained. There was no difference in the distribution of labeled neurons between $Sinc^{s7}$ and $Sinc^{p7}$ mice, i.e., between mice differing in the amino acid sequence of their PrP proteins. Therefore, although high levels of PrP are detected in a variety of cell types in other organs (13), in brain, PrP is a largely a neuronal protein. This is in agreement with *in situ* hybridization studies that have shown that the *Prnp* gene is expressed predominantly in neurons (14).

Patterns of PrP Accumulation with Different Strains of Scrapie

Extensive accumulation of PrP was seen in all scrapie models. Several different forms of PrP-related pathology were apparent (5), the most usual being a widespread accumulation in the neuropile; this appeared as coarsely granular deposits against a background of more diffuse immunolabeling. In some areas of brain without this extensive neuropile pathology, there was a scattered fine punctate labeling of the neuropile that was not obviously associated with any particular cell type; although these structures had the size and appearance of neuronal processes, it was not possible to identify them positively as such. Amyloid plaque cores, which were frequent in some models, were also strongly immunostained. Immunoreactivity was seen often within microglia and rarely within astrocytes; in some models, many astrocytes were surrounded by an ill-defined halo of PrP. However, the most striking cellular association was seen as intense labeling around particular individual neurons and their cell processes (5). This had a similar appearance to the perineuronal β/A4 accumulations reported by Probst and coworkers in Alzheimer's disease (15).

There were dramatic and remarkably reproducible differences between scrapie strains in their patterns of PrP-related pathology (5) (Fig. 1). Scrapie strains differed in the relative prominence of the above changes and in their distribution in the brain. The pathology was very similar for different mouse strains of the same *Sinc* genotype infected with a single scrapie strain. For ME7, the pathological characteristics were compared in $Sinc^{s7}$ and $Sinc^{p7}$ mice (Fig. 1A,B); the distribution and details of PrP accumulation were indistinguishable in the two genotypes.

With 87V in $Sinc^{p7}$ mice, diffuse and granular neuropile accumulation was targeted precisely to particular areas, leaving much of the brain clear apart from prominent amyloid plaques and scattered punctate changes (Fig. 1C). In many parts of the brain, there was a clear association of diffuse neuropile pathology with particular groups of neurons and their processes. Most obviously, in the hippocampus there was a clear preferential involvement of an area corresponding exactly to the dendritic field of the pyramidal neurons of the CA2 sector. Accumulation of PrP around individual neurons, unobscured by more widespread neuropile pathology, was particularly obvious in the lateral hypothalamus in this model.

In contrast, the ME7 strain in both $Sinc^{s7}$ and $Sinc^{p7}$ mice produced PrP accumulation throughout the neuropile in most areas of brain, although some areas were predictably more severely affected than others (Fig. 1A,B). There were also large numbers of plaques, but these tended to be smaller and had less obvious amyloid cores than those seen with 87V. A striking pathological feature seen with ME7, but not with 87V or 79A, was a characteristic zonal pattern of PrP accumulation in the molecular layer of the cerebellum (16); labeling appeared as stripes that were perpendicular to the cerebellar surface, and were similar in appearance and location to the diffuse β/A4 cerebellar plaques reported in Alzheimer's disease (17). Often with ME7 scrapie, these stripes were continuous across several folds of the cerebellum, suggesting a link with the longitudinal zonal organization of the mammalian cerebellum, that is based on projections of Purkinje cells to vestibular and cerebellar nuclei (18). This, in turn, suggests that this type of pathology is associated with the Purkinje cells, more specifically with their dendrites. Perineuronal PrP accumulations were also seen in the lateral hypothalamus and elsewhere with ME7, but these tended to be obscured by diffuse neuropile deposits.

The 79A scrapie strain in $Sinc^{s7}$ mice also produced widespread PrP accumulation, affecting most parts of the brain, but the distribution was different from that of ME7 (Fig. 1D). Labeling was less intense than with the other two strains and was qualitatively different, having a more diffuse, less granular appearance. Plaques were small and infrequent. Many astrocytes were surrounded by a diffuse PrP halo, and rarely, PrP could be demonstrated within

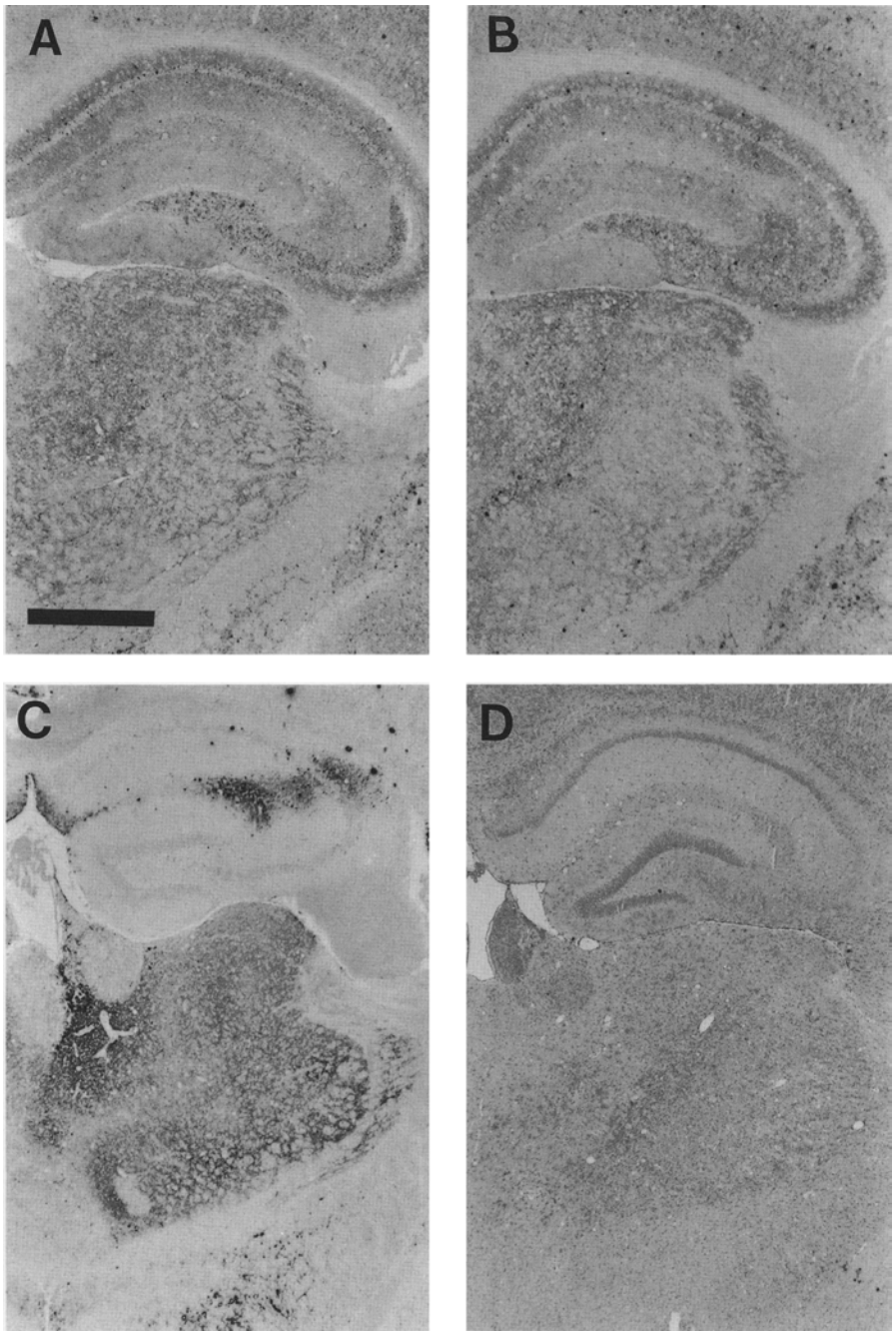

Fig. 1. Sections of thalamic and hippocampal brain areas, immunostained with antiserum to PrP. **(A)** *Sinc*^{s7} mouse infected with ME7 scrapie strain, **(B)** *Sinc*^{p7} mouse with ME7 scrapie, **(C)** *Sinc*^{p7} mouse with 87V scrapie, and **(D)** *Sinc*^{s7} mouse with 79A scrapie (bar = 1 mm).

astrocytic cell bodies. Although hypertrophied astrocytes were seen within areas of diffuse accumulation in all models, this specific astrocytic association was not seen with 87V or ME7. However, the astrocytic involvement with 79A was similar to that reported by Diedrich and coworkers (and confirmed in our own laboratory) for the 22L strain of scrapie *(19)*.

Table 1
Timing and Location of First Abnormalities in PrP Distribution in Three Intracerebral Scrapie Models

Scrapie strain	Mouse genotype	Incubation period, d	Time of first PrP changes, d	Sites of first PrP changes
ME7	*Sinc*^{s7}	182	35	Medial geniculate nucleus
87V	*Sinc*^{p7}	320	80	Substantia nigra/locus ceruleus
79A	*Sinc*^{s7}	146	34	Median raphe/septohippocampal nuclei

The results with 87V and ME7 strongly suggest that the primary target cell for scrapie infection is the neuron, and that accumulating PrP is produced by neurons. They also suggest that different strains of scrapie recognize and target infection and resulting pathology to different groups of neurons. The marked differences between models in the involvement of astrocytes remain to be explained.

Serial Studies of PrP Accumulation

PrP changes were first seen relatively early, between a fifth and a quarter of the way through the intracerebral incubation period, depending on the model, and many weeks before the development of vacuolar degeneration (Table 1). Abnormal distributions of PrP appeared at about the time that relatively protease-resistant PrP became detectable by Western blotting *(20)*. Even at this early stage, scrapie strains showed clear preferences for particular brain areas. Abnormalities were first seen in these areas on the side of the intracerebral injection, progressing to give a widespread symmetrical pathology later in the incubation period.

The first detectable change in PrP distribution in all models was the appearance of intensely immunostained scattered dot-like structures in the neuropile *(5)*. Although microglia and astrocytes became involved at an early stage, the first changes were not associated with either cell type; this was true even for 79A, which later showed a very prominent astrocytic involvement. It is likely that the location of these first PrP changes reflects the early replication of agent within the brain. Amyloid plaques were also seen at an early stage, but only in areas adjacent to the lateral ventricles. Because plaques are not seen in this site following intraperitoneal injection and inoculum is disseminated through the ventricles immediately following an intracerebral injection, it has been suggested that periventricular plaques in intracerebrally injected mice are related to foci of replicating agent, originating from direct local infection by the inoculum *(21)*.

Ultrastructural Localization of PrP

The subcellular localization of PrP was investigated in *Sinc*^{p7} mice infected intracerebrally with the 87V strain of scrapie *(11)*. This model was chosen because it produces several different forms of PrP accumulation that appear morphologically distinct at the light microscopy level. Blocks were collected from areas of brain known to contain widespread diffuse and granular neuropile deposits, amyloid plaques, or perineuronal accumulations. Precise areas were selected from immunostained 1-μ*M* araldite sections, examined by light microscopy, and adjacent 65-nm sections were immunogold-labeled for electron microscopy. There was a close correlation between immunolabeling patterns at the light and ultrastructural levels.

As expected, amyloid fibrils in plaque cores were decorated with gold particles. Immunogold labeling was also seen in the plaque periphery where there were no detectable amyloid fibrils; here an increased frequency of gold particles was associated with the plasmalemma of neuronal processes or the adjacent extracellular space. A similar labeling of neurite plasmalemma was seen within areas of neuropile and perineuronal PrP accumulation (Fig. 2). Morphometric analysis of the distribution of gold particles in low-power electron micrographs confirmed these observations. There was about ten times the density of gold particles on neurite plasmalemma and extracellular space than elsewhere in the micrographs *(11)*.

Pathological features of scrapie, such as vacuoles, dystrophic neurites, and tubulovesicular bodies, were all seen within the areas of PrP accumulation, but none were specifically labeled. Reactive microglia and astrocytes were also frequent, but were unlabeled apart from occasional lysosomal staining within microglia. Furthermore, some immunolabeled areas, for example in perineuronal sites, showed no significant abnormality of tissue structure or organization. Since PrP is normally a neuronal cell membrane protein and accumulation

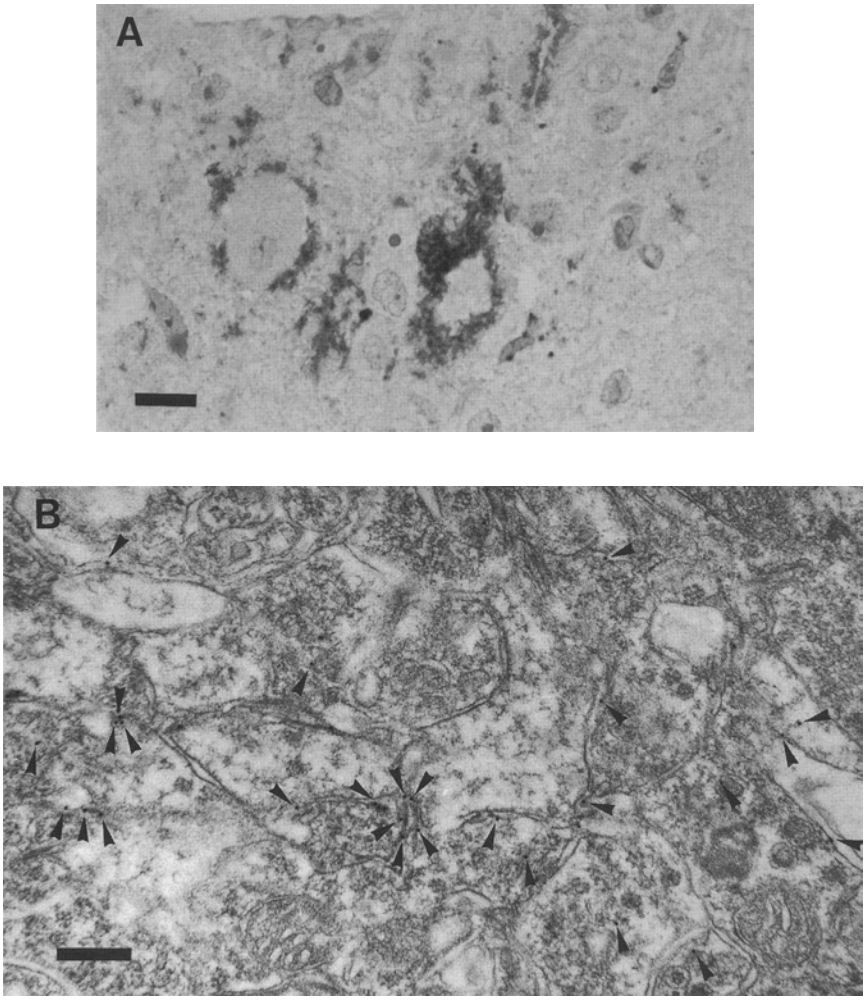

Fig. 2. **(A)** Perineuronal immunostaining of PrP in araldite section from brain of *Sinc*^{p7} mouse with 87V, viewed by light microscopy (bar = 20 μm). **(B)** Electron micrograph showing immunogold labeling of PrP in a perineuronal site in the same model, with gold particles indicated by arrows. The majority of gold particles are located on the plasmalemma of neurites surrounding the neuronal cell body (bar = 200 nm).

appears to occur at the surface of neurons and their processes, the simplest interpretation is that conversion of normal PrP to its infection-specific form also occurs at the neuronal cell surface.

Role of PrP in Pathogenesis

It has been known for many years that the *Sinc* gene controls the incubation period of scrapie in mice *(7)*. To define the action of the *Sinc* gene in more detail, the replication of ME7 scrapie was followed through the incubation period in *Sinc*^{s7} and *Sinc*^{p7} mice, using the intraocular route of infection *(12)*. Following intraocular injection, infection is delivered precisely and with predictable timing to the terminals of the retinal ganglion cell axons within the superior colliculus. Levels of infectivity in this area were measured at intervals through the incubation period, by incubation period assay. It was found that the *Sinc* gene controlled the onset, rather than the rate of replication (Fig. 3). Since the *Sinc* gene probably encodes PrP, this result suggests that PrP may be involved in the cell-to-cell spread of infection rather than the actual replicative process. Such a role would be consistent with the association of normal PrP with the cell surface and the fact that PrP accumulates pathologically at the neuronal plasmalemma.

Our current understanding of scrapie pathogenesis is that infection spreads through the CNS along neural pathways, that neuron-to-neuron spread

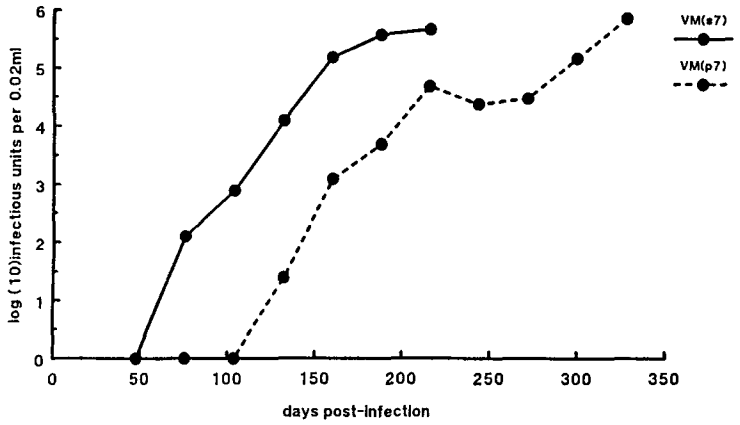

Fig. 3. Sequential titer estimates from pools of superior colliculi taken from $Sinc^{s7}$ and $Sinc^{p7}$ mice following intraocular infection with ME7 scrapie. Tissues were taken at 48, 76, 104, 132, 160, 188, and 216 d from $Sinc^{s7}$ mice and additionally at 244, 272, and 300 d from $Sinc^{p7}$ mice *(11)*.

occurs at or near the synapse, and that this spread is restricted by the relative permissiveness to infection of the neurons in the relay *(22)*. Although it is probable that host PrP controls the overall rate of this process, possibly by controlling cell-to-cell spread, it is not clear whether this protein is involved in the selective targeting of infection to particular groups of neurons. We have shown that the primary structure of host PrP has no consistent effect on lesion type and distribution; with ME7, the patterns of PrP accumulation in the two genotypes are indistinguishable. Nevertheless, it remains possible that different posttranslationally modified forms of normal PrP exist in different populations of neurons, and that these provide cues for recognition and selection by different scrapie strains. Alternatively, targeting could depend on any of the many other molecules that are known to define neuronal populations, the most obvious being neurotransmitters and related molecules, including receptors.

The molecular nature of the scrapie agent also remains a matter for speculation. On the one hand, the failure so far to identify scrapie-specific nucleic acids and the fact that PrP and infectivity tend to copurify in extracts from infected tissues have led to the suggestion that modified PrP itself is the scrapie pathogen *(23)*. On the other hand, no specific modifications of PrP have been identified that can account for strain variation, and it is difficult to construct theoretical models in which the protein alone can specify strain diversity. Whatever the molecular nature of the agent, it is clear from the studies described here and in a large number of previous investigations that scrapie strains carry some form of information that is independent of the host, but that closely controls the ways in which the pathogen interacts with the host. It is also clear that host PrP plays a major role in this interaction.

Summary

PrP accumulation in the brains of mice infected with scrapie takes several different forms: amyloid plaques, widespread accumulation in neuropile, and perineuronal deposits. PrP is also sometimes detected within microglia and in or around astrocytes. There are dramatic and reproducible differences between scrapie strains in the relative prominence of these changes and their distribution in the brain. Depending on the scrapie strain, PrP pathology is targeted precisely to particular brain areas, often showing a clear association with identifiable groups of neurons. These results suggest that PrP changes are primarily associated with neurons, and that different scrapie strains recognize and selectively replicate in different populations of neurons. Immunostaining at the ultrastructural level demonstrates an association of PrP with neurite plasmalemma, around amyloid plaques, and in areas of widespread neuropile and perineuronal accumulation. It is probable that PrP is encoded by the *Sinc* gene, which controls the incubation period of scrapie in mice. Studies using the intraocular infection route show that the *Sinc* gene controls the onset rather than the rate of replication, suggesting that PrP may be involved in cell-to-cell spread of infection. The accumulation of PrP at the surface of neurons is consistent with such a role.

Acknowledgments

The authors would like to thank John Brown and Caroline Goodsir for excellent technical assistance.

References

1. McKinley M. P., Bolton D. C., and Prusiner S. B. (1983) *Cell* **35,** 57–62.
2. Merz P. A., Somerville R. A., Wisniewski H. M., and Iqbal K. (1981) *Acta Neuropathol. (Berl.)* **54,** 63–74.
3. Prusiner S. B., Bolton D. C., Groth D. F., Bowman K. A., Cochran S. P., and McKinley M. P. (1982) *Biochemistry* **21,** 6942–6950.
4. DeArmond S. J., Mobley W. C., DeMott D. L., Barry R. A., Beckstead J. H., and Prusiner S. B. (1987) *Neurology* **37,** 1271–1280.
5. Bruce M. E., McBride P. A., and Farquhar C. F. (1989) *Neurosci. Lett.* **102,** 1–6.
6. Bruce M. E., McConnell I., Fraser H., and Dickinson A. G. (1991) *J. Gen. Virol.* **72,** 595–603.
7. Dickinson A. G., Meikle V. M. H., and Fraser H. (1968) *J. Comp. Pathol.* **78,** 293–299.
8. Westaway D., Goodman P. A., Mirenda C. A., McKinley M. P., Carlson G. A., and Prusiner S. B. (1987) *Cell* **51,** 651–662.
9. Hunter N., Dann J. C., Bennett A. D., Somerville R. A., McConnell I., and Hope J. (1992) *J. Gen. Virol.* **73,** 2751–2755.
10. Farquhar C. F., Somerville R. A., and Ritchie L. A. (1989) *J. Virol. Meth.* **24,** 215–221.
11. Jeffrey M., Goodsir C. M., Bruce M. E., McBride P. A., Scott J. R., and Halliday W. G. (1992) *Neurosci. Lett.* **147,** 106–109.
12. Scott J. R., Davies D., and Fraser H. (1992) *J. Gen. Virol.* **73,** 1637–1644.
13. McBride P. A., Eikelenboom P., Kraal G., Fraser H., and Bruce M. E. (1992) *J. Pathol.* **168,** 413–418.
14. Manson J., McBride P., and Hope J. (1992) *Neurodegeneration* **1,** 45–52.
15. Probst A., Langui D., Ipsen S., Robakis N., and Ulrich J. (1991) *Acta Neuropathol. (Berl.)* **83,** 21–29.
16. Bruce M. E., McBride P. A., Jeffrey M., Rozemuller J. M., and Eikelenboom P. (1993) *Alzheimer's Disease: Advances in Clinical and Basic Research* (Corain B., Iqbal K., Nicolini M., Winblad B., Wisniewski H. M., and Zatta P. F., eds.), Wiley, Chichester, pp. 481–487.
17. Yamaguchi H., Hirai S., Morimatsu M., Shoji M., and Nakazato Y. (1989) *Acta Neuropathol. (Berl.)* **77,** 314–319.
18. Voogd J., Gerritts N. M., and Marani E. (1985) *The Rat Nervous System, Vol. 2: Hindbrain and Spinal Cord* (Paxinos G., ed.), Academic, Sydney, pp. 251–291.
19. Diedrich J. F., Bendheim P. E., Kim Y. S., Carp R. I., and Haase A. T. (1991) *Proc. Natl. Acad. Sci. USA* **88,** 375–379.
20. Farquhar C. F., Dornau J., Somerville R. A., Turnstall A. M., and Hope J. (1994) *J. Gen. Virol.* **75,** 495–504.
21. Bruce M. E. (1981) *J. Comp. Pathol.* **91,** 589–597.
22. Kimberlin R. H. and Walker C. A. (1986) *Unconventional Virus Diseases of the Central Nervous System* (Court L. A., Dormont D., Brown P., and Kingsbury D. T., eds.), Commissariat a l'Energie Atomique, Fontenay-aux-Roses, pp. 547–562.
23. Prusiner S. B. (1982) *Science* **216,** 136–144.